

An Atlantic influence on evapotranspiration in the Orinoco and Amazon basins

Nicolás Duque-Gardeazabal^{1,2}, Andrew R. Friedman^{1,2,3}, and Stefan Brönnimann^{1,2}

¹Oeschger Centre for Climate Change Research, University of Bern, Bern, Switzerland.

²Institute of Geography, University of Bern, Bern, Switzerland.

³now at Laboratoire de Météorologie Dynamique / Institute Pierre-Simon Laplace, Paris, France

Correspondence: Nicolás Duque-Gardeazabal (nicolas.duque@unibe.ch)

Abstract.

Tropical South America's hydroclimate is influenced by ocean-atmospheric variability modes (drivers of climate variability). It is still not known which physical mechanisms teleconnect the Atlantic modes of variability with South America's soil moisture, net radiation and terrestrial evaporation (evapotranspiration). Understanding these mechanisms is essential for predicting the response of ecosystems. This study uses composites of reanalysis and satellite data to identify the processes linking land-surface anomalies and ocean-atmospheric modes. It estimates the control soil moisture and net radiation impose over evapotranspiration (categorised as water- or energy-limited regimes). It shows that these two local controllers of evapotranspiration are influenced by the position of the Intertropical Convergence Zone (ITCZ). However, the evapotranspiration anomalies are driven by the phase of each climate mode which alter water and radiation availability. The Atlantic Meridional Mode (AMM) generates cross-equatorial wind anomalies that affect moisture convergence, in turn modifying the cloud cover, precipitation, soil moisture, radiation availability and hence evapotranspiration. The anomalies have important geographical differences depending on the analysed season; they migrate from the east in Austral autumn towards central Amazon and western Orinoco in Austral spring. The Atlantic Niño Equatorial mode (Atl3) affects evapotranspiration in the Guianas and eastern Orinoco by means of pressure and trade wind variability, which in turn affect local hydrometeorological conditions and evapotranspiration. Both Atlantic modes mainly impact regions different from those impacted by El Niño/Southern Oscillation (ENSO), although northeast Brazil and the Guianas might experience overlapping effects. Therefore, these ocean-atmospheric modes impact the water, energy and carbon cycles and might influence regional climate extremes (e.g. droughts and floods), and are critical for achieving sustainable development (SDG).

Copyright statement. TEXT

1 Introduction

The hydroclimate of tropical South America is strongly influenced by ocean-atmospheric variability modes (climate drivers), for instance, El Niño/Southern Oscillation (ENSO) (Cai et al., 2020; Garreaud et al., 2009; Grimm and Zilli, 2009). Other

sources of seasonal variability stem from other ocean basins (e.g. the Atlantic, Indian Ocean, etc), and at other temporal scales from Madden-Julian Oscillation or local features like topography or land-atmosphere interactions (Pabón and Dorado, 2008; Cai et al., 2019). The modes cause impacts through atmospheric circulation anomalies and hence drive local atmospheric conditions; the latter enforces hydrological variability, which is evidenced by anomalies of precipitation, soil moisture (SM), surface temperature, evapotranspiration and streamflow. The atmospheric anomalies might also influence extreme events (e.g. droughts and floods)(Merz et al., 2021; Mishra and Singh, 2010), and their consideration in long-term planning is critical for achieving sustainable development.

Among the hydrological fluxes, terrestrial evaporation is key for water, energy and carbon cycles (Wang and Dickinson, 2012). This flux mainly consists of evaporation from soil, interception and plant transpiration (hereafter all jointly referred as evapotranspiration - ET). Limitations in ET influence growth processes and hence carbon uptake, previous studies have linked net primary or biome production variability to SM-atmosphere feedbacks and climate/earth system drivers, e.g. through climate-driven droughts (Nemani et al., 2003; Humphrey et al., 2021; Zhao and Running, 2010). There is evidence that individual extreme weather events can coerce plant phenology, for instance on flowering, leaf senescence and plant growth (Ummenhofer and Meehl, 2017). Therefore, to predict ecosystems' activity, it is essential to identify the mechanisms of internal climate variability drivers that enforce a response in ET. Moreover, estimating the response of ET to climate variability drivers is also necessary for unravelling the effects of climate change on hydrology (IPCC, 2021), and for estimating irrigation requirements (Kaune et al., 2019).

In the following, we consider oceanic variability modes in the Pacific and Atlantic as drivers of the climate variability in the Amazon and Orinoco basins (Lübbecke et al., 2018). Some studies statistically looked at the Pacific and Atlantic joint effects on precipitation (Gu and Adler, 2009; Ronchail et al., 2002). Others studied the interannual changes in moisture transport dynamics – imposed by oceanic climatic drivers – and their associated rainfall anomalies over South America (Hoyos et al., 2019; Ruiz-Vásquez et al., 2024). Atlantic trade winds strength and the precipitation anomalies are related to ocean variability modes such as: the Tropical North Atlantic mode (TNA)(Arias et al., 2015, 2020; Enfield, 1996), the Atlantic Meridional Mode (AMM) (Chiang et al., 2002; Fernandes et al., 2015; Rodrigues and McPhaden, 2014; Paccini et al., 2021; Drumond et al., 2014) and the Atlantic Niño Equatorial mode (Atl3) (Ruiz-Barradas et al., 2000; Torralba et al., 2015; Vallès-Casanova et al., 2020). The Atlantic modes tend to be active and peak between the Austral autumn and spring – MAM, JJA and SON (the initial letters of the months) – contrary to ENSO which peaks at the end of the year (SON and D(0)JF(+1)). These Atlantic modes might have contributed to northeast Brazil droughts and the Magdalena River floods in 2011-2012, as well as the Amazon droughts in 2005 and 2010 (Lopes et al., 2016; Marengo and Espinoza, 2016). Although the Atlantic modes are associated with ENSO through atmospheric bridges or extratropical pathways (Compo and Sardeshmukh, 2010; Martín-Rey et al., 2014; García-Serrano et al., 2017; Casselman et al., 2023), each of them has specific regional impacts on sea-level pressure (SLP) and hence on atmospheric circulation.

However, the variability of evapotranspiration has received less attention than precipitation. Previous research has established SM and Net Radiation (Rn) as the primary local controllers of ET (Seneviratne et al., 2010; Hirschi et al., 2014); consequently, ET is classified into two regimes: water- or energy-limited. The annual cycle and the location of the regimes are

not known in South America and are important for understanding ET variability. Some studies have statistically investigated the teleconnections of ENSO (Moura et al., 2019; Le and Bae, 2020; Miralles et al., 2014) or other climate drivers with the ET around the world (Martens et al., 2018), but the physical causes for these connections are not known. Specifically, it is not known how the interannual changes in moisture transport impact net radiation. In our paper, we focus on the Atlantic modes, which have received less attention in the literature. Moisture recycling is another factor that can impact surface radiation, but previous studies have focused on its impact on regional and distant precipitation rather than radiation (Staal et al., 2018; Wang-Erlandsson et al., 2018; Zemp et al., 2014; van der Ent and Savenije, 2011). Other research has looked at the influence of Amazon soil moisture memory on ET (Zanin et al., 2024) or how anomalous moisture transport from the TNA affects SM and vegetation indices (Arias et al., 2020), but other Atlantic modes have been overlooked.

Consequently, it is still not known how the variations in regional atmospheric circulation – driven by the Atlantic modes – alter local continental atmospheric conditions and afterwards affect net surface radiation and soil moisture, the two key local controllers of ET. We refer to the latter as the physical mechanisms of the teleconnection, which consist of a chain of progressive physical processes. Ecological processes respond to the variability of hydrometeorological conditions (Eagleson, 2013); by understanding the mechanisms leading to that variability, the community can increase the potential predictability of ecosystems' activity. Therefore, this study aims to investigate the physical causes of the link between the AMM and Atl3 with ET in tropical South America, at seasonal scale. Other drivers, such as the Indian Ocean Dipole mode, the Atlantic Multidecadal Oscillation (AMO), etc., are excluded from our study (see Sect. 3 and 5). Moisture recycling is only briefly discussed in Sect. 5. We aim to answer the following questions:

1. Where and in which season is the evapotranspiration dominated by a water- or energy-limited regime?
2. How do the Atlantic modes drive anomalous atmospheric circulation and influence the variability in local atmospheric conditions, and how do they then affect the local controllers and thus affect evapotranspiration?
3. Where do the dynamics and, thus, the impacts of the Atlantic modes overlap with those of ENSO in time and space?

2 Data

This study uses net radiation, soil moisture (SM) and ET, as well as atmospheric circulation variables, such as SLP, winds, moisture transport, convergence and rainfall. We use those atmospheric variables because ocean-atmospheric modes drive the regional atmospheric circulation, which afterwards influences the local ET controllers. Sea Surface Temperature Anomalies (SSTAs) are used to identify the ocean-atmospheric modes (Sect. 3). All datasets are downloaded at monthly time scale and used between Dec-1979 and Nov-2020 (except for satellite-based soil moisture, details in Sect. 2.2); they are aggregated at seasonal scale and analysed for each season individually and synchronously. The aggregation method for all variables is the average of the three monthly values, except for precipitation and ET when we use the sums (Duque-Gardeazabal, 2025).

Satellite and reanalysis data sources each have strengths and limitations. Satellite data can provide some of the needed data mainly over land but moisture transport is not available from this source. Reanalysis data are considered physically-based

90 interpolations of observations and provide atmospheric variables that satellites do not directly acquire. Satellite-based datasets have difficulties in measuring soil moisture over densely forested canopies (Beck et al., 2021). Errors in the root zone SM compromise the estimation of plant water stress and, thus, the skill of the ET estimate. On the other hand, simulations of ET which ingest reanalysis outputs might inherit their biases (Gebrechorkos et al., 2024; Valencia et al., 2023). Although the performance of both data sources has improved in recent years (Beck et al., 2021; Xie et al., 2024), their estimates remain
95 uncertain, and confidence in their inter-annual dynamics rests on the fact that the analysed signals are evident in independent datasets. Therefore, we look for consistency in the dynamics of both sources of information; we do not regrid and do not merge any datasets because we do not perform operations between them. We display the datasets conjointly when necessary and analyse the dynamics unfolding in both data sources (Table 1).

We use SSTAs from the Extended Reconstructed SST version 5 (Huang et al., 2017) – which is used as the primary dataset
100 – and the Hadley Center Sea Ice and SST version 4.0.1 (Kennedy et al., 2019). ERSST is at 2°, and HadSST is at 5° resolution.

2.1 Reanalysis

The ECMWF ERA5 reanalysis provides information on atmospheric variables that influence the local controllers of evapo-
transpiration and also relates to the dynamics of the coupled ocean-atmospheric modes (Hersbach et al., 2020). Monthly time series of winds, Vertically Integrated water vapour Flux (VIMF), mean SLP and vertically integrated Moisture flux Divergence
105 (MDiv) are taken from it. All atmospheric variables from ERA5 have 0.25° spatial resolution.

ERA5-Land is a land-surface simulation operationally forced by ERA5, which includes detailed modules on infiltration, four-layer physically-based soil water storage, plant water-uptake, phenology and transpiration, and evaporation from soil and canopy interception (Muñoz-Sabater et al., 2021; ECMWF, 2023). From it, we download or derive the net surface radiation (Rn), the volumetric soil water content in the first soil layer (hereafter soil moisture - SM) and the total evaporation (hereafter
110 also referred to as evapotranspiration - ET). All variables from ERA5-Land have 0.1° resolution.

2.2 Satellite

This research uses the Multi-Source Weighted-Ensemble Precipitation v2.8 (MSWEP)(Beck et al., 2019) with a spatial resolution of 0.1°. The dataset is created with rain gauges, satellite and reanalysis data. MSWEP uses ERA5 rainfall estimates mainly in the extratropics, whereas the ingested satellite data is given stronger weight in the tropics.

115 In addition we use three satellite-based datasets: the European Space Agency Climate Change Initiative for Soil Moisture v08.1 (ESI-CCI-SM) (Gruber et al., 2019), total evaporation from the Global Land Evaporation Amsterdam Model v3.8a (GLEAM) (Martens et al., 2017), and the EUMETSAT CLARA-A3 cloud area fraction as a proxy of net radiation (Karlsson et al., 2023), all of them at 0.25° resolution. ESA-CCI-SM was downloaded at daily resolution and transformed to monthly values by averaging the days within each month as long as the month had at least four values; the remaining spatial gaps
120 were not filled and were excluded from calculations. GLEAM uses a three-layer conceptual root zone soil module from which vegetation can access water (which considers ESA-CCI-SM assimilation where available). It includes a module for plant stress

Table 1. Overview of the datasets used in this study. ERA5 is described in Hersbach et al. (2020), ERA5-Land in Muñoz-Sabater et al. (2021) and ECMWF (2023)

Variable	Reanalysis			Satellite		
	Dataset	Spatial resolution	Temporal resolution	Dataset	Spatial resolution	Temporal resolution
Sea Level Pressure	ERA5	0.25°	Monthly	-	-	-
Winds at 850 hPa	ERA5	0.25°	Monthly	-	-	-
Vertically Integrated						
Water Vapor Flux (VIMF)	ERA5	0.25°	Monthly	-	-	-
Moisture Divergence (MDiv)	ERA5	0.25°	Monthly	-	-	-
Precipitation	-	-	-	MSWEP v2.8 (Beck et al., 2019)	0.1°	Monthly
Net Surface Thermal Radiation	ERA5-Land	0.1°	Monthly	CLARA-A3 Cloud Area Fraction	0.25°	Monthly
Net Surface Solar Radiation	ERA5-Land	0.1°	Monthly	(Karlsson et al., 2023)		
Soil Moisture (volumetric water content 1st soil layer)	ERA5-Land	0.1°	Monthly	ESA-CCI-SM v08.1 (Gruber et al., 2019)	0.25°	Daily (Aggregated to Monthly)
Total Evaporation	ERA5-Land	0.1°	Monthly	GLEAM v3.8a (Martens et al., 2017)	0.25°	Monthly
Sea Surface Temperature Anomalies		ERSST v5 (Huang et al., 2017)			2°	Monthly
		HadSST v4.0.1 (Kennedy et al., 2019)			5°	Monthly

based on SM and vegetation phenology, and it also provides evaporation from interception and bare soil. GLEAM uses ERA5 radiation as forcing.

Some eddy-covariance towers are located in the Amazon and other places in South America; their measurements are –in general– after 2000. Baker et al. (2021) managed to use records from one tower with 19 years of data (1999-2017) but highlighted that in the other towers the data was only available for a few years (mainly between 1999 and 2006). Other global products based on FLUXNET towers, such as FLUXCOM (Jung et al., 2019), also have data after 2001. The short time series constrains the possibility of registering several events to analyse the effect of the climate modes (few degrees of freedom). The performance of GLEAM and ERA5-Land ET have been evaluated against eddy-covariance towers and have found correlations

130 of around 0.6 and 0.7 for the Evergreen Broadleaf Forest ecoregion, respectively (Muñoz-Sabater et al., 2021; Xie et al., 2024). Therefore, we choose not to analyse eddy-covariance data and assume a fair performance of the other two sources.

3 Methods

Climate modes and their atmospheric circulation anomalies are expected to impact evapotranspiration through a chain of progressive physical processes. The processes start with anomalies in atmospheric circulation (coupled with SSTA), and moisture transport (VIMF). Then, the latter changes moisture flux divergence (MDiv), affecting cloud formation; which simultaneously influences precipitation and radiation availability. Precipitation then affects soil moisture, and afterwards, the two local controllers impact evapotranspiration. However, the impacts of the chain are also mediated by the climatological cycle of the ET regime (water- or energy-limited). Consequently, our research starts by determining the annual cycle of the ET regime and of the local controllers (section 3.1). Then, we use composites to show how the chain unfolds with its final impacts on ET (section 140 3.2). Finally, we study the joint effects of the Atlantic modes and ENSO (section 3.3)(Duque-Gardeazabal, 2025). Moisture recycling is discussed in section 5.

3.1 Determining the location and annual cycle of local ET controllers

This study explores the two main local controllers of ET (soil moisture and net radiation) (Seneviratne et al., 2010), to afterwards search for the ocean-atmospheric modes that drive those controllers. SM and net radiation are classified with the slope of their multi-linear regression against evapotranspiration, using their seasonally standardised anomalies. This analysis can suggest whether the ET anomalies are associated with water availability or a radiation anomaly (ET regime). The multiple linear regression is then expressed as:

$$ET_{ij} = a_{ij} * SM_{ij} + b_{ij} * Rn_{ij} + C \quad (1)$$

Where ET is the total evaporation, SM is the volumetric soil water content in the first layer, Rn is the surface net radiation, i refers to a specific longitude and j to a specific latitude. a and b are then the regression slope coefficients and C the intercept. 150

3.2 Composites

This study uses composite analysis to exemplify the state of the atmosphere and the land surface at the active phase of the Atlantic modes. The composites reveal the physical processes/mechanisms that connect the variables.

Coupled ocean-atmospheric modes are identified with SSTA indices. The SSTA are first detrended to exclude the effect of climate change from the analysis using a regression with de-seasonalised CO_2 ($R^2 = 0.92$, $p < 0.001$) (Thoning et al., 1989); the CO_2 concentration is used to consider its continuous change in the 20th and 21st century and to avoid subtracting the internal variability. We performed Principal Components Analysis over the detrended Atlantic SSTA and the resulting loadings were compared with the literature review (Fernandes et al., 2015; Vallès-Casanova et al., 2020; Ruiz-Barradas et al., 2000)(supplementary Figure S8). Correlation analysis between the principal components and hydrological variables revealed

160 which modes possibly have an impact on South America (not shown). Other climate modes, such as the Indian Ocean Dipole, the AMO, etc., unfold over basins that are not close to our study area, and hence, they do not alter tropical South America's atmospheric circulation. Consequently, we discard them from our analysis. We define the Atlantic indices based on SSTA area-average boxes similar to the principal component loadings of the Atlantic SSTs (Figure S8).

- The AMM monthly index is defined as the difference between the spatially averaged tropical north Atlantic (TNA) SSTA
165 [70°W-15°W]x[5°N-25°N] and the tropical south Atlantic (TSA) [40°W-0°W]x[25°S-5°S]; the spatial definition of the AMM comprises the TNA.
- The Atl3 monthly index is identified as the spatial average of eastern equatorial Atlantic SSTAs [20°W-0°]x[3°S-3°N].

To define the composite time steps, the phases of each mode are established based on the indices. The positive and negative phases are identified when their indices are above or below ± 1 standard deviation, respectively, and otherwise are defined as
170 neutral phase. The latter is defined individually for each season (indices time series in Figure S8). The asymmetric impacts of the modes are assessed by adding both extreme phases (positive plus negative), allowing the recognition of the different impacts exerted by each phase. The composite's statistical significance is assessed with the two-sample Student's two-tailed T-test, testing positive or negative phase against the neutral. Regarding precipitation, half of the cell's time series have skewed distributions (Shapiro-Wilk test; not shown). Thus, the Mann-Whitney U test is used instead. We did not find a significant
175 correlation of evapotranspiration with CO_2 . Nevertheless, ET time series are detrended with a linear trend to also exclude global warming (Zhang et al., 2016), before being used in the composites.

ENSO develops in the second semester and its peak season is DJF. On the other hand, the AMM is more active from February onwards but might last until SON (Yoon and Zeng, 2010), and the Atl3 is more active in JJA (Vallès-Casanova et al., 2020). In DJF, the AMM-associated anomalies are evident over the Atlantic but its effect over the continent is diluted (not shown).
180 Therefore, we analyse the influence of the Atlantic modes from March to September.

3.3 Conjoint effect with ENSO

We also perform grid-wise partial correlation analysis between the two Atlantic indices, the El Niño Longitude Index (ELI)(Williams and Patricola, 2018), and evapotranspiration. The ELI considers the type of ENSO event (east or central Pacific). The purpose of this analysis is to find those regions that are driven by an Atlantic mode but might also have impacts from another mode
185 when it is also active (i.e. simultaneously controlling the analysis by the effect of ENSO and the other Atlantic mode).

4 Results

4.1 Key local evapotranspiration controllers

The classification of the ET regime follows the migration of the Intertropical Convergence Zone (ITCZ, located in the south Amazon in DJF and over north Orinoco in JJA)(Fig. 1). The reason is associated with the heavy rainfall of the ITCZ which

190 saturates the soils and influences the locations of the energy-limited regime. Panels a to h in Figure 1 show the slope coefficients of the regressions, which are then ranked in panels i to l. Values below 0 indicate that the other independent variable is the main controller of ET. In MAM (Fig. 1a,e,i), the north-easterly winds bring moisture from the Atlantic and produce convergence and rainfall over the Amazon in such an amount that the soil saturates (and thus is above the soil's water field capacity), giving the conditions for an energy-limited ET. However, the north of the Orinoco basin still behaves as a water-limited environment.

195 As the ITCZ moves northward in JJA (Fig. 1b,f,j), the rainfall recharges SM, changing Orinoco's behaviour to energy-limited, whereas other regions transform from energy- to water-limited regimes like northeast Brazil, as well as the south Amazon. The core of the Amazon rainforest is energy-limited throughout the year. In SON (Fig. 1c,g,k), the ITCZ begins to move southward, but the energy-limited regime is concentrated in the west of the Amazon. The east and southeast basins are still in a water-limited regime. The Orinoco still behaves as energy-limited even though this is the transition season from wet to dry. In DJF

200 (Fig. 1d,h,l), the ET in the south Amazon depends on the available energy as the ITCZ is on its southern continental location; above-average net radiation (R_n) would produce more ET. The energy-limited regions correspond to those where SM is above the soil's field capacity (ECMWF, 2023)(not shown), and not all the continent is primarily controlled by variations in energy supply.

4.2 Chain of physical processes between the Atlantic modes and continental evapotranspiration

205 This section shows the composites of the variables involved in the chain (see Section 3). The steps in the chain repeat as far as a mode is active. However, the impacts have important geographical differences depending on the mode and the season analysed.

4.2.1 March - May (MAM) Austral Autumn

The Atlantic Meridional Mode (AMM) consists of a SST and SLP seesaw between the Tropical North and South Atlantic, creating cross-equatorial wind anomalies (see Figure S1 for SLP and 850 hPa winds composites). In Austral autumn, the positive

210 phase redirects and advects moist air northward, towards the Orinoco, where it provokes positive convergence and precipitation anomalies (Fig. 2a). The location of the satellite precipitation and reanalysed convergence anomalies are consistent between both datasets. The positive convergence creates more clouds that then reduce net surface radiation (Fig. 2c). Soil moisture (SM) is impacted by the anomalous rainfall; Figure 2e shows that the SM anomalies in northern Orinoco are sensitive to the AMM in positive phase. ESA-CCI-SM is available for this region and shows similar dynamics (Fig. S2). The western and southern

215 Amazon have SM anomalies lower than absolute 2% as it is the rainy season and the soil is near saturation.

The evapotranspiration is afterwards impacted. The Orinoco behaves as water-limited (Fig. 1i) since this is the transition from dry to wet season, then the increase in rainfall and SM causes above-average ET (Fig. 2g). Over northeast Brazil, the positive phase produces divergence anomalies and less cloud cover (Fig. 2a and c). The latter increases radiation but enforces higher evapotranspiration than average due to the high SM availability above the soil's field capacity which allows the region

220 to act as energy-limited (Fig. 1i and 2g). GLEAM independently shows similar results over northern Orinoco – more extended increase in ET – but over northeast Brazil the area with increased ET is smaller than in ERA5-Land and is surrounded by negative anomalies (Fig. S3). We will examine the box area-averaged time series in Figure 6.

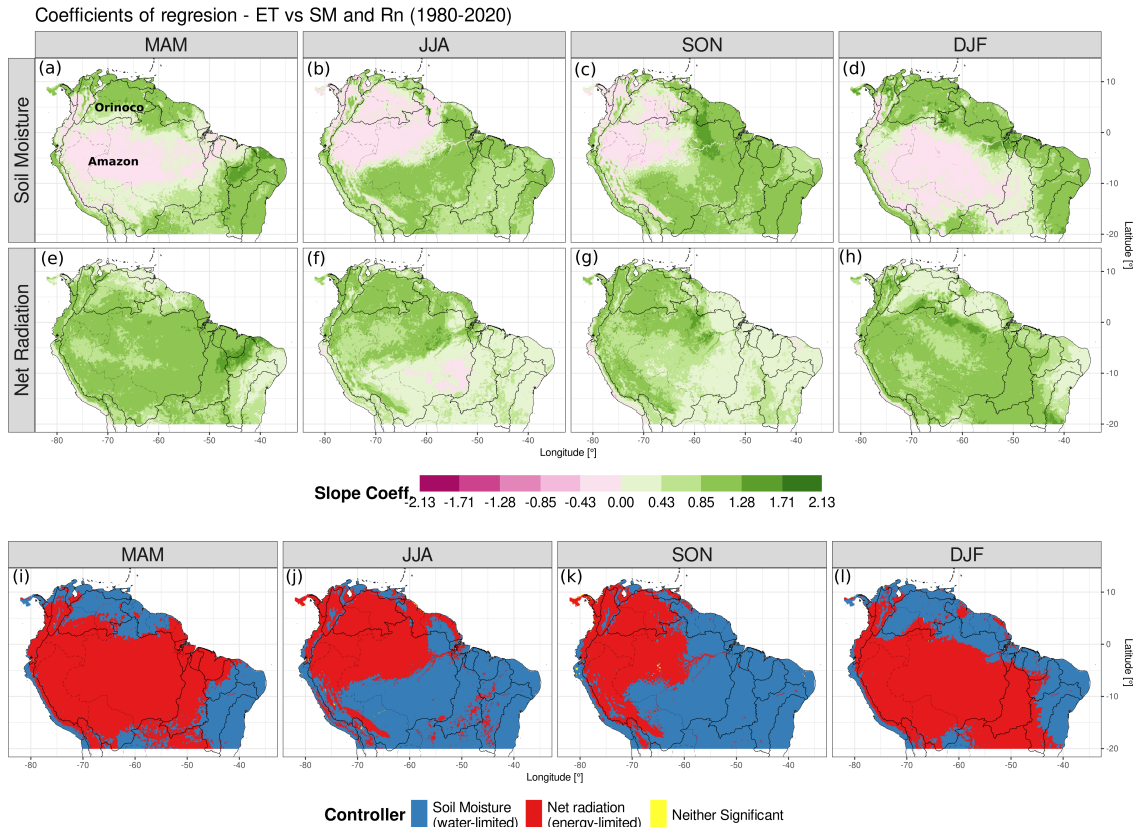


Figure 1. Classification of ERA5-Land evapotranspiration (ET) controller based on regression coefficients for each season. (a-d) multiple linear regression slope coefficient for soil moisture (SM), (e-h) slope coefficient for the net radiation (Rn) and (i-l) variable with the highest significant linear slope coefficient ($p \leq 0.05$). Panels are divided by the seasons (a,e,i) for MAM, (b,f,j) for JJA, (c,g,k) for SON and (d,h,l) for DJF. Black lines delineate the major river basins; the same boundaries are used in the following figures.

In the negative phase, the AMM redirects the VIMF southward towards northeast Brazil (Fig. 2b). The anomalous winds generate greater moisture convergence, which reduces radiation and then ET over that region (Fig. 2b,d and h). Over the northern Orinoco, the southward moisture advection causes a reduction in rainfall and below-average SM, further limiting ET. The eastern Amazon evapotranspiration is not affected like in the positive phase (asymmetry). However, GLEAM estimates show that in northeast Brazil the impacted area is not as big as in ERA5-Land and does not show ET anomalies where the ESA-CCI-SM was unable to detect values (Fig. S2 and S3).

Comparing positive and negative phases, the mode shows asymmetric atmospheric circulation, with the negative phase being stronger in magnitude for the VIMF (Fig. S7). The latter causes a decrease in SM over the northeast Amazon that is higher than the increase in the positive phase, considering absolute values. Regarding ET, some regions are affected only in one phase of the mode, such as the eastern Amazon and its river delta.

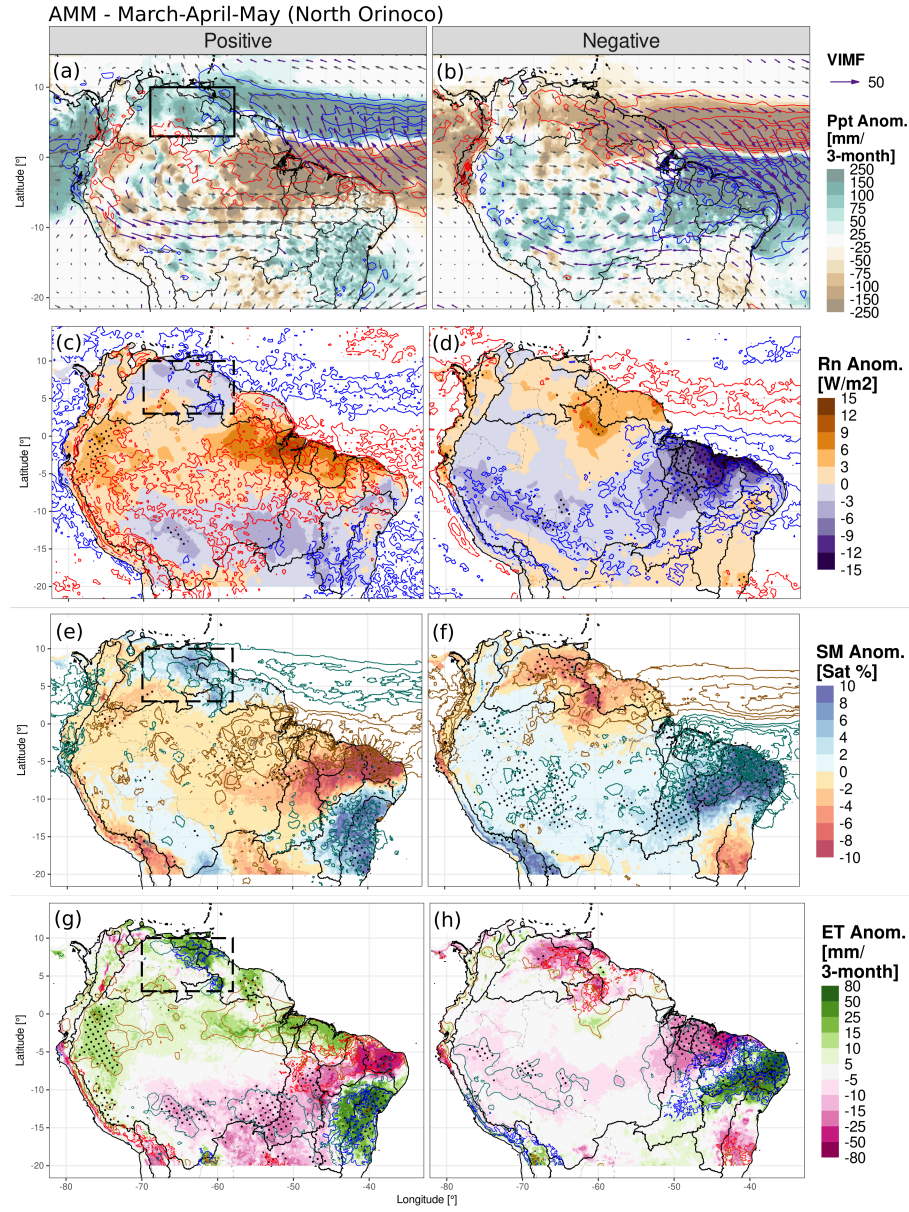


Figure 2. Anomaly composites of AMM in MAM for (a) VIMF (arrows), MDiv (contours) and MSWEP precipitation (shading) anomalies in the positive phase; positive MDiv anomalies are in red and negative in blue every 3 kg/m^2 . VIMF is in kg/m/s and depicted in purple when it is statistically significant at a 90% confidence level and in grey otherwise. Right panels (b,d,f and h) are the same as left panels (a,c,e and g) but for the negative phase. (c,d) ERA5-Land surface net radiation (shading), and satellite CLARA cloud cover anomalies (contours); positive cloud cover anomalies are in blue and negative in red repeated every 4%. (continue in next page)

Figure 2. (continued.) (e,f) Composites of ERA5-Land soil moisture anomalies in saturation percentage (shadings), and MSWEP precipitation anomalies (contours); positive precipitation anomalies are drawn in aquamarine and negative in gold repeated every 100 mm. (g,h) Composites of ERA5-Land evapotranspiration (shading), Rn anomalies (contours, gold for positive and aquamarine for negative), and SM anomalies (contours, blue for positive and red for negative); Rn anomalies are repeated every 3 W/m^2 and SM anomalies are repeated every 5%. In every panel, black stippling depicts regions where the shaded variable is significantly different at a 95% confidence level with respect to the neutral phase. Boxed region: Northern Orinoco, also applies for the negative phase.

4.2.2 June - August (JJA) Austral Winter

The Atlantic Niño (Atl3) is characterised by a decrease in SLP and an increase in SST over the equatorial east Atlantic that usually peaks in JJA (Fig. S1). It weakens the trade winds through the Bjerknes feedback with effects over VIMF and precipitation over the continent (Fig. 3a). SM and evapotranspiration are not extensively impacted by the Atl3 positive phase as changes in radiation are barely visible (Fig. 3c, e and g). The Atl3 impacts are not clear in other seasons (SON and DJF) when the AMM and ENSO exert a more discernible influence (not shown).

Conversely, stronger JJA trade winds increase Ekman pumping and mixing over the Atlantic and manifest as colder SST (known as Atlantic Niña – Atl3 negative phase). The strengthened easterly winds – and VIMF – create negative anomalies of convergence and precipitation in an extended region over the East of the continent (Fig. 3b). However, greater MDiv and radiation increase ET over the eastern Orinoco and the Guianas due to the energy-limited environment, whereas over northeast Brazil and the eastern Amazon the anomalies are negative as they behave as water-limited and the SM is also lower-than-average (Fig. 1j and 3d,f,h). ESA-CCI-SM is not available over the Guianas and partially over northeast Brazil (Fig. S2) and then GLEAM shows a similar pattern to ERA5-Land, but the signal is weaker over the eastern Orinoco, Amazon delta and northeast Brazil (Fig. S3). The negative phase is more pronounced due to stronger anomalies in all three variables (Figure S7 for asymmetric conditions). The ET between the two phases is very asymmetric as the eastern Orinoco and northeast Brazil are not affected in the positive phase, but they are in the negative (Fig. 3g and h, and Fig. S7).

Regarding the Atlantic Meridional Mode (AMM) (Fig. 4), the impacted place migrate depending on the season. In JJA, the positive phase redirects the VIMF anomalies northward (Fig. S4). This enhances convergence over the Caribbean and the divergence over the central Amazon and southern Orinoco (the latter having enhanced convergence in the previous season); hence, it reduces clouds and rainfall over the continent (Fig. S4 a and c). The SM levels guarantee an energy-limited environment in the northern Amazon (Fig. 1j), and the AMM-related divergence generates above-average radiation, causing higher-than-average ET in the tropical forest (Fig. 4c) but below-average over northeast Brazil. The places impacted migrate westward compared to the previous season - MAM (Fig. 4a). In the southern area, the combination of the dry season and below-average SM cause trees to uptake water probably just through their deep roots, generating water stress and reduced ET (see Sect. 5 Discussion). However, GLEAM estimates do not show any significant anomaly in the Amazon where the availability of ESA-CCI-SM estimates are scarce (Fig. S2 and S3). Both ET datasets show similar anomalies over the continental north coast.

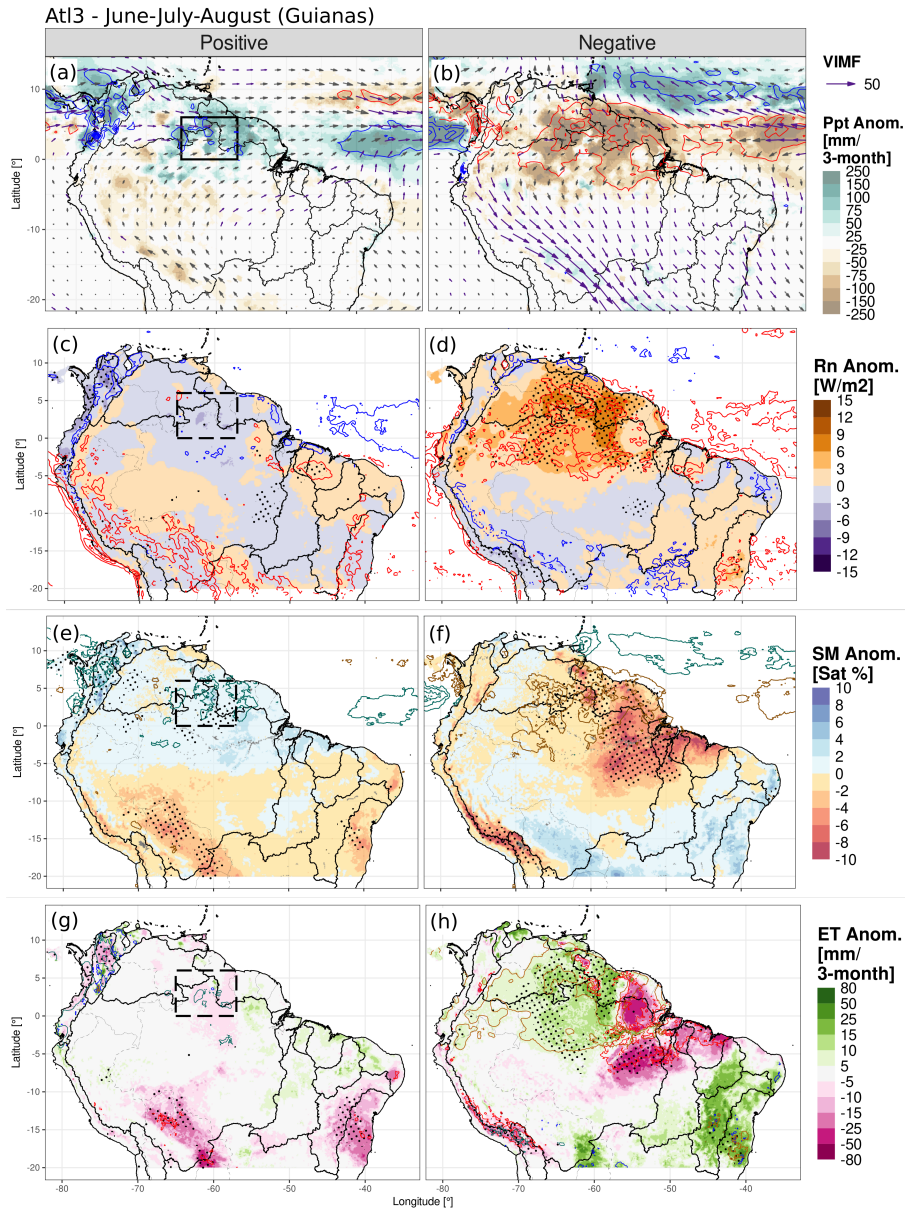


Figure 3. As in Figure 2 but for the Atlantic Niño Equatorial Mode (Atl3) in June to August (JJA). Boxed region: Guianas, also applies for the negative phase.

In the JJA negative phase, southward moisture flux brings more rainfall to the Orinoco but it is not clear over the Amazon, an asymmetric condition compared to the positive phase (Fig. S4). Then, the AMM negative phase produces positive but not significant SM and ET anomalies in the southeast (Fig. 4d), although ERA5 suggests enhanced convergence (Fig. S4b). An

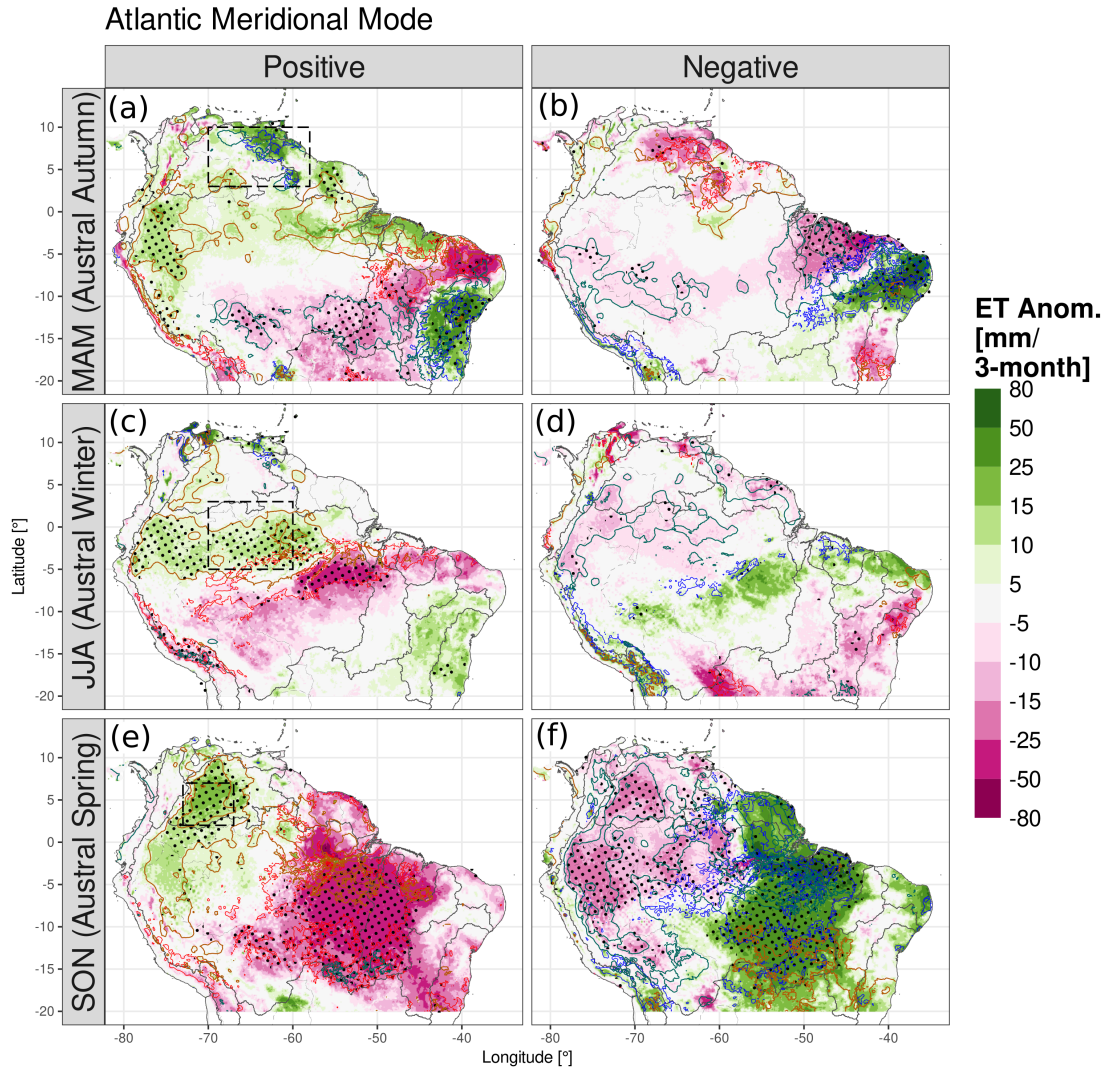


Figure 4. Anomalies of ERA5-Land ET (shadings) in the positive and negative Atlantic Meridional Mode (AMM) phases, for seasons (a,b) March-May, (c,d) June-August, (e,f) September-November. Positive phase in panels (a,c,e) and negative (b,d,f). Net surface radiation anomalies are in contours (gold for positive and aquamarine for negative), as well as soil moisture anomalies (contours, blue for positive and red for negative); radiation anomalies are repeated every 3 W/m^2 and SM anomalies are repeated every 5%. Black stippling depicts regions where the difference with the neutral phase is statistically significant at a 95% confidence level. Boxed regions: (a,b) Northern Orinoco, (c,d) Central Amazon, (e,f) Western Orinoco, also applies for the negative phase. Box-averaged time series for JJA and SON in Figure S6.

important difference comparing JJA to MAM is the westward migration of the divergence anomalies from northeast Brazil to the central Amazon and the effects on SM and ET (Fig. 4a and c).

4.2.3 September - November (SON) Austral Spring

265 For this season, the AMM-related anomalies migrate to the western Orinoco and western Amazon since the rainfall is concentrated on the Andes' eastern slope. The reduction of VIMF and convergence in the positive phase leads to high radiation anomalies that interact with the SM, causing above-average ET over the Orinoco (Fig. 4e and S5a,c,e). This is generated by SM remaining high in the region, creating an energy-limited environment although it is not the core of the rainy season and the SM anomalies are less than 2% (Fig. 1k and Fig. S5e). Moreover, the positive phase causes a decline in SM and ET over the
270 water-limited southeast due to the reduction of rainfall. There is no significant change in central northern Amazon, just in the west or the east.

In the negative phase, the AMM brings extra moisture more strongly than the positive phase, although in both phases the southeastern Amazon is impacted (Fig. S5a,b and S7). In the latter region, the SM shows higher-than-average values (Fig. S5e), which grant the land surface the extra moisture to increase ET in the water-limited zone (Fig. 4f). Over the Orinoco, the reduced
275 radiation causes less ET but also over the western and northern Amazon (the latter region not affected in the positive phase, asymmetry Fig. S7). GLEAM shows similar results except for the central Amazon, again a region where the satellite SM is not assimilated in the model (Fig. S2 and S3).

The interactions between SM availability, plant water uptake and radiation lead – in some cases – to above-average evapotranspiration during negative precipitation anomalies (reduced moisture convergence and clouds). This behaviour is present in
280 energy-limited regimes, whereas in water-limited environments, negative moisture convergence anomalies bring less rainfall and cause below-average evapotranspiration.

4.3 Atlantic modes connection with ENSO and impacts on evapotranspiration

Both ENSO and the Atlantic modes are connected through tropical and extra-tropical mechanisms, but each of them have effects on South American hydroclimate. Figures 5 and 6, separate the effects of each mode in the spatial and temporal dimensions,
285 respectively.

ENSO and AMM have impacts on ET at similar but also over different locations depending on the analysed season. Figures 5a,b,e,f show the influence of both modes on ET in northeast Brazil in MAM and in JJA, yet ENSO mainly impacts the eastern Amazon and the AMM the Orinoco (see Sect. 5 Discussion). ENSO usually also induces droughts in the Amazon during El Niño events – mostly during its peak season DJF – and causes heavy rainfall and floods in La Niña events. Figure 5(c,d) shows
290 the spatial impact of the increased evapotranspiration during ENSO-driven droughts and Figure 6(c,d) displays the impacts on rainfall and ET of specific events (e.g. 1983, 1992, 1997 and 2015). However, Figures 5(a,e) and 6(a,b) show that in the northern Orinoco the ENSO forcing might be superseded by the meridional moisture advection induced by the AMM (e.g. 1983 – El Niño year but higher rainfall and ET; 1985 and 1989 – La Niña year but drought). The correlation of the AMM with rainfall is up to 0.64, and with SM and ET are up to 0.5, all significant. Another period when the AMM superseded ENSO
295 impacts was in La Niña 2010 when the central Amazon experienced a prolonged drought (Fig. 5f and S6); the cause was the positive AMM event (see Sect. 5 Discussion). Note also the reduction or increment of ET when SM changes (water-limited

regime). For season SON (Fig. 5 c and g), the AMM and ENSO tend to impact different regions, ENSO being strong over the Guianas and the AMM over the west and southeast.

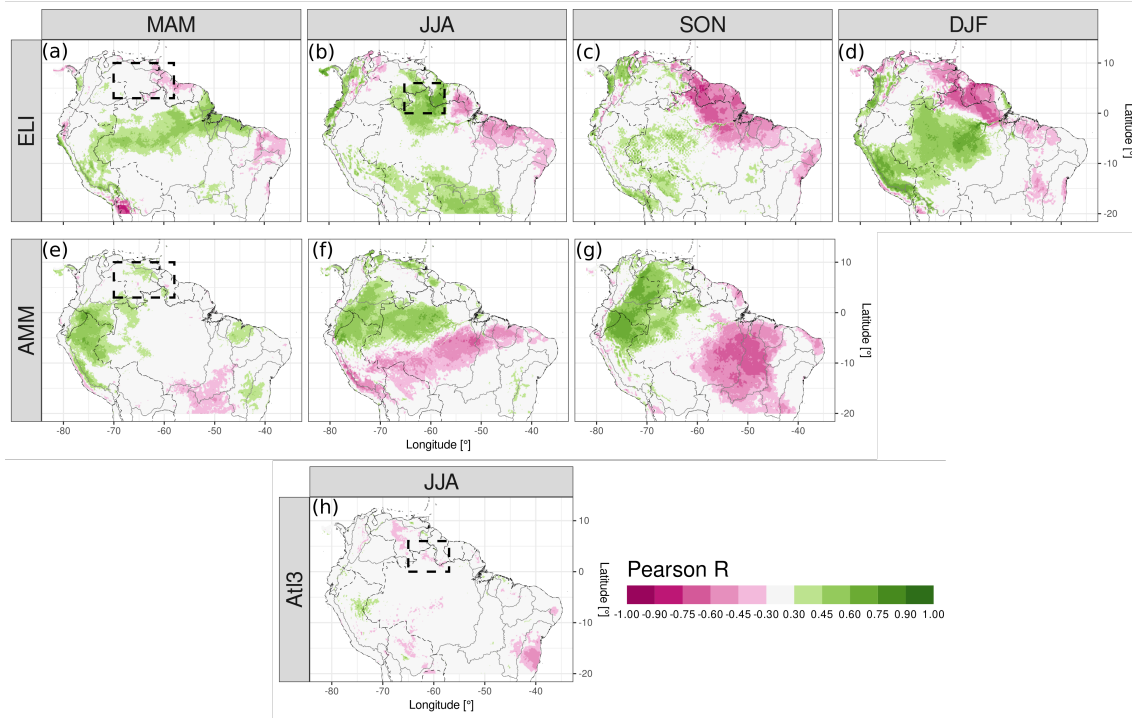


Figure 5. Partial correlation of ET from ERA5-Land with the main tropical ocean modes in the Atlantic and Pacific. Panels a-d are the correlations with ELI for each season, controlling by the two Atlantic indices, e-g are the correlations with the AMM except for DJF controlling by ELI and Atl3, and panel h is the correlation with the Atl3 controlling by ELI and the AMM. Just 95% confidence level values are shown in colours. Boxed regions: Northern Orinoco and Guianas, same as in Fig.2 and 3.

The Atl3 does not seem to strongly correlate with ET over the Guianas, and the ENSO pattern for JJA is very similar to the
 300 Atl3 negative phase composites (Fig. 5b,h and 3h). This indicates some overlapping dynamics between the two modes, which are probably more associated with the atmospheric dynamics of El Niño phase that has simultaneously unfolded with the Atl3 negative phase (Fig. 6c and d and Fig. S8). We discuss the latter in Section 5. Figure 6c and d show the droughts over the northeast Amazon and Guianas at Atl3 negative events with the corresponding increase in ET, also expected effects of El Niño phase. The correlation of the Atl3 with the area-average ERA5-Land ET is -0.46 but 0.14 with GLEAM; the index correlates
 305 well with SM and also with rainfall. However, only some Atl3 positive events significantly reduced radiation and ET in the region (e.g. 1988, 1999 and 2008); other events kept ET close to the average (1987, 1998 and 2016).

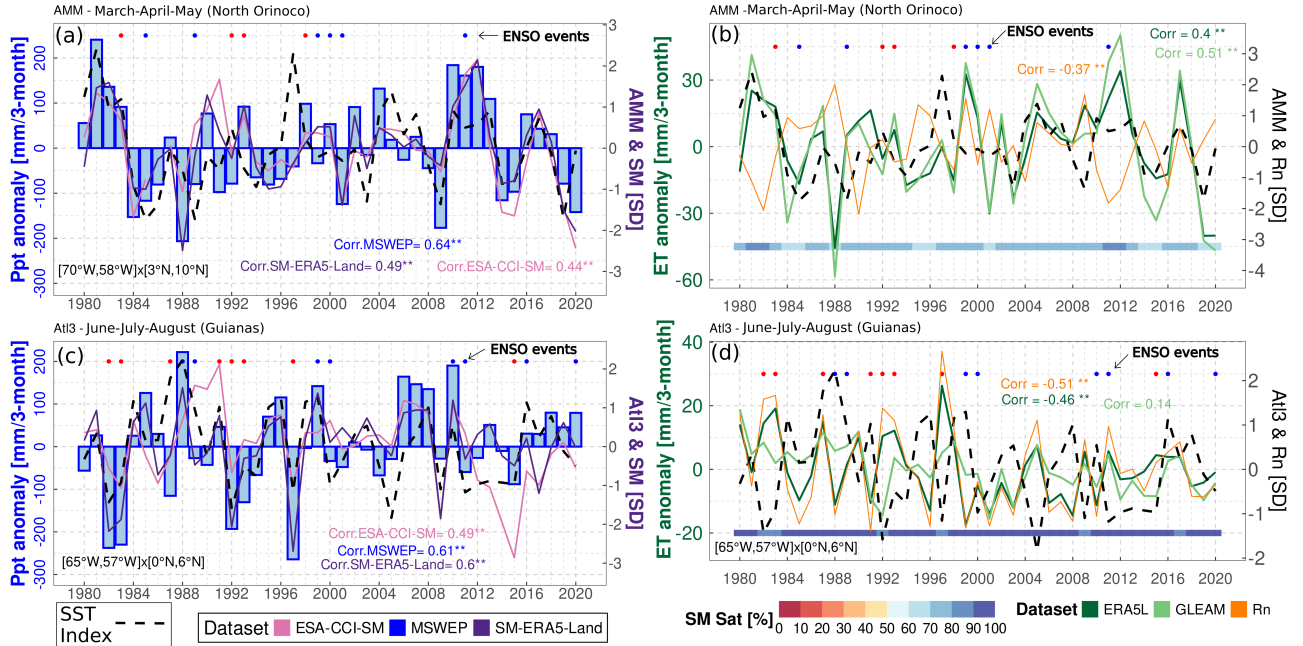


Figure 6. (a,c) Area-average precipitation (bars) and SM standardised anomalies time series (lines) for the same boxes in Figure 2 and 3, respectively; the Atlantic index time series is in black dashed lines in standard deviation (right axis), and top points show ENSO active periods (positive phase in red and negative in blue). (b,d) Area-average evapotranspiration time series (greens), ERA5-Land net surface radiation (orange), standardised Atlantic index (black dashed) and ERA5-Land absolute SM in saturation percentage at the bottom of the panel with coloured rectangles. For the same boxes of panels (a) and (b). For all panels, Pearson correlations are calculated between the variable – either precipitation, SM, Rn or ET – with the respective Atlantic index, 95% confidence level is indicated with **. Boxed regions: Northern Orinoco (a and b); Northeast Amazon and Guianas (c and d).

5 Discussion

Much of the research has focused on precipitation variability rather than on evapotranspiration (Arias et al., 2021; Marengo and Espinoza, 2016; Poveda et al., 2006; Espinoza et al., 2011). Regarding ET, Martens et al. (2018) used machine learning to globally estimate the impacts of the AMM – and other modes – finding the increased evapotranspiration over northeast Brazil in MAM and some cells in the central Amazon in JJA. However, our research focused on the modes that alter the atmospheric circulation close to the continent and constitute the physical mechanism causing the teleconnection. Other investigations focused specifically on ENSO's impact on Amazon evapotranspiration and SM (Moura et al., 2019; Poveda et al., 2001). Specifically, Moura et al. (2019) showed the anomalies of evapotranspiration for both south Amazon's rainy – DJF – and dry seasons during ENSO events, finding the increase in the ET also shown in our correlation analysis in DJF. Our research focuses on the interaction between the atmosphere and the land surface, finding that the impacts migrate from the eastern Amazon to the western Orinoco and that important asymmetries exist between phases. Hasler and Avissar (2007) found an increase

in ET in the equatorial Amazon during the dry season related to radiation anomalies, as found in our ERA5-Land composites. The retained SM above critical values (soil's field capacity), up to the next season, might cause positive evapotranspiration anomalies during below-average precipitation and above-average radiation periods (Zanin et al., 2024); this is evident in our results in the transition from the wet to the dry season.

Differences between GLEAM and ERA5-Land stem from their formulation structures and assimilated data, which are then propagated to the composite analysis. In forested areas, roots deeper than 1.5 m allow the water uptake from deep layers as a survival mechanism (Roberts et al., 2005; O'Connor et al., 2019; Jarvis, 1976), the main local controller of ET is most likely the incoming radiation but trees might still feel water stress (Lian et al., 2024). The latter is partially considered in ERA5-Land as the depth of the last layer is deeper than 1.5 m and plants withdraw soil moisture root-percentage-wise (ECMWF, 2023), whereas in GLEAM the three soil layers depth is not specified and plants withdraw water from the wettest layers (Martens et al., 2017). D'Acunha et al. (2024) found low ET rates in cropland and pasture sites inside the southeast Amazon rainforest compared to natural land use; the structure of both datasets in our study considers the grasslands and the other land covers, with some limitations. The influence of wind speed on evapotranspiration is not considered in GLEAM v3.8, and the soil module and plant physiology are more accurate in ERA5-Land. The impediment of assimilating SM due to the scarcity of ESA-CCI-SM data in dense forest areas might compromise the uncertainty in GLEAM estimates (Baker et al., 2021), e.g. over the northern Amazon and Delta, and over the Guianas (Fig. 4d,e and 5d,e). Some studies have compared both datasets against eddy-covariance towers and water-balance approaches and concluded that ERA5-Land estimates are more realistic than GLEAM (Muñoz-Sabater et al., 2021; Xie et al., 2024). The bias in ERA5's rainfall might be diverted towards the streamflow (Towner et al., 2021), rather than generating a bias on the SM and the ET. These limitations are probably the main cause of the differences between the composites using each dataset.

The variability of ET has implications for moisture-recycling, mainly for southeastern South America as pointed out by Drumond et al. (2014). Although moisture recycling inside the Amazon comprises between 25% and 35% of rainfall, Dominguez et al. (2022) discovered that it is a short-lifetime phenomenon strongly linked to the diurnal cycle of advected moisture and convection; recycled moisture precipitates quickly. Staal et al. (2018) measured the distance of transpired water before precipitating again over land, finding that for the particles transpired in the Amazon, the distance is below or around 500 km (which is short for the size of the Amazon basin). Our results show the places that affect the sources of that moisture recycling due to the seasonal aggregated increments or reductions in ET. Makarieva et al. (2023) determined the influence of ET on moisture convergence, which potentially might influence radiation. It remains to be clarified to what extent moisture-recycling influences radiation availability and soil moisture at other locations in South America; the latter is out of the scope of our research.

The AMM and the Atl3 are influenced by and also have feedback with ENSO (García-Serrano et al., 2017; Martín-Rey et al., 2014; Cai et al., 2019). Our results show that each mode impacts different regions, except for northeast Brazil and north Amazon where they overlap through El Niño enforcing convection inhibition and the AMM producing meridional anomalous moisture advection (for instance, in 2010)(Chiang et al., 2002; Arias et al., 2020); these mechanisms then modify convergence, rainfall, radiation availability and thus evapotranspiration. The AMM negative phase has been less recurrent in SON in the last decades associated with a positive phase of the Atlantic Multidecadal Oscillation (AMO)(general interhemispheric temperature

gradient) (Brönnimann et al., 2015; Friedman et al., 2020). The latter is apparently related to the reduced aerosol forcing over the northern hemisphere and its associated radiation scattering (Hua et al., 2019; He et al., 2023). The Atl3 negative phase has co-occurred with the ENSO positive phase (El Niño)(Münnich and Neelin, 2005), whose impacts are evident in our composites and partial correlation analysis. ENSO causes downward atmospheric movement over the east of the Amazon that hampers convection and precipitation (Cai et al., 2020); simultaneously, the strengthened easterlies – typical of the negative Atl3 – add to the moisture divergence over the Guianas, undermining precipitation. However, the relationship between ENSO and the Atl3 is inconsistent (Chang et al., 2006; Lübbecke and McPhaden, 2012). The interactions between climate modes have implications for their continental impacts (i.e. over the hydrological cycle).

Several ocean-atmospheric drivers have been identified to influence the hydrometeorology of South America. Rodrigues and McPhaden (2014) analysed the AMM effects on precipitation in northeast Brazil and the Amazon, while others focused on the decadal variations of precipitation and streamflow or the low atmospheric dynamics (Fernandes et al., 2015; Lopes et al., 2016; Olmo et al., 2022). Our research shows that the chain of events starts with the SSTA and SLP and transfers to VIMF, MDiv and precipitation, whose anomalies are linked to the variability of ET. However, we also show that the AMM also affects the Orinoco basin in MAM, JJA and might even extend into SON (Yoon and Zeng, 2010), not just over the Amazon and precipitation but also over the SM and the evapotranspiration. There is agreement in the comparison of the location of reanalysed convergence and satellite precipitation; the rainfall anomalies influence peak river flow, and our results agree with the location of peak river flow reduction during TNA anomalies reported by Towner et al. (2021) – decrease in central Amazon in the positive phase. Regarding the Atl3, most of the studies have focused on its statistical relationship with continental precipitation anomalies (Gu and Adler, 2009; Torralba et al., 2015), and the atmospheric dynamics of its development (Vallès-Casanova et al., 2020).

Although coupled ocean-atmospheric modes are important drivers at seasonal time scale as shown here, other sources of variability at other scales – such as those mentioned in Sect. 1 Introduction – influence precipitation and might also influence ET (Mariotti et al., 2018). They might affect the transition and migration of the anomalies from one season to the following one. Phenomenons with longer frequencies, such as the AMO, have also been discussed here, but the impacts of all those sources on ET deserve further research.

Our results are underpinned by the consistency between independent observations of land-surface and atmospheric variables whose robustness comes from physically-based interpolations (reanalysis) or satellite-based observations. Limitations arise from the dataset's uncertainty and satellite retrievals; deforestation dynamics are also not included in the datasets. Nevertheless, the general circulation is still well represented due to the assimilation of atmospheric pressure, and models and measurements are as accurate as possible. Both sources of information show similar impacts but with local differences mostly in densely forested areas where physically based models like ERA5-Land might be more reliable. Longer time series of eddy-covariance towers could help the community confirm the dynamics discovered in our study. All in all, the datasets are accurate enough to analyse interannual variability.

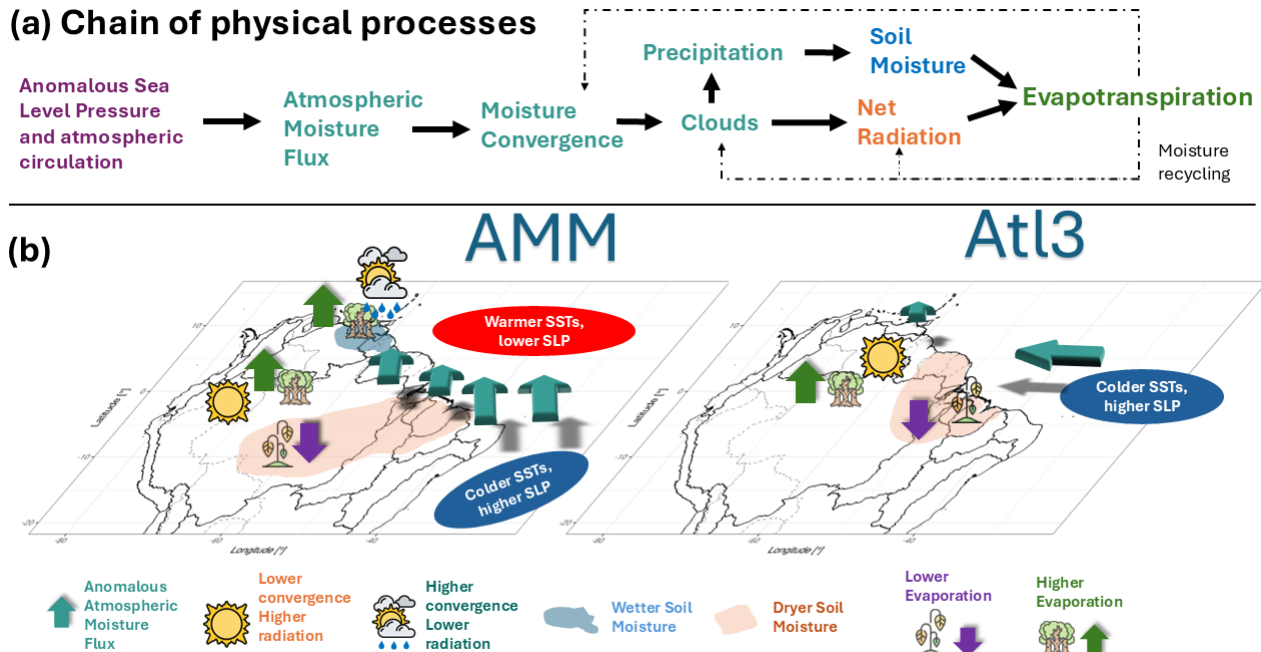


Figure 7. Schematic figure of the (a) variables involved in the chain of physical processes in the teleconnection between a climate mode and the evapotranspiration. (b) Geographical location of the processes involved in the connection between the continental evapotranspiration and the Atlantic Meridional Mode (AMM), and the Atlantic Niño Equatorial mode (Atl3).

6 Conclusions

This research advances the current understanding of the physical mechanisms that cause the interannual climate and land-surface variability in Tropical South America, focusing on soil moisture (SM), net radiation (Rn) and evapotranspiration (ET). It elucidates the influence of the Atlantic SST modes on upwind conditions that impact the Orinoco basin and not just northeast Brazil or the Amazon. Atlantic ocean-atmospheric interactions drive moisture convergence anomalies, in turn, modifying water and radiation availability, which then control the SM, the net radiation and ET anomalies. However, the chain of processes is modulated by the annual cycle of the evapotranspiration regimen which is not completely energy-limited throughout the tropical region and throughout the annual cycle. A summarising depiction of the processes can be seen in Figure 7.

The Atlantic Niño Equatorial mode (Atl3) weakens the trade winds in JJA, producing convergence over the Guianas and eastern Orinoco. However, its effect on the SM, radiation and ET is not strong. The negative phase – in conjunction with ENSO El Niño – strengthens the trade winds and produces divergence over an extended region which significantly changes the SM, Rn and ET.

The Atlantic Meridional Mode (AMM) creates cross-equatorial SLP anomalies that deflect climatological winds not just over the ocean but also over the continent. It retrieves moisture northward on the positive phase, on occasions increasing and

400 in others reducing convergence, precipitation and radiation depending on location and season, hence causing the land-surface anomalies (SM and ET). The negative phase causes the contrary effect but with strong asymmetries. In MAM, the moisture is redirected towards the Orinoco from northeast Brazil, whereas in JJA and SON it is taken from south Orinoco and north Amazon (or brought to the same regions in the other phase with important differences in zonal direction). The changes in moisture transport depend on the annual wind pattern, producing opposite effects when comparing MAM and JJA over the
405 Orinoco. AMM and ENSO conjointly affect the breadbasket region of northeast Brazil and the central Amazon but the AMM affects more the western Amazon and Orinoco.

The regions impacted in each phase might be different. Analysing just one phase might cause misleading estimations in SM, Rn and ET.

Evapotranspiration is not only influenced in its regime by the ITCZ position but also by the phase of the ocean-atmospheric
410 mode. This is related to the fact that SM is not resilient to the activation of the modes unless it is the rainy season when in whatever phase the soil is saturated (and thus the SM is above the soil's water field capacity, threshold for energy-limited ET). For instance, evapotranspiration anomalies in the transition season from wet-to-dry are energy-limited, but the sign of the anomaly depends on the phase of the mode which alters radiation and then ET. In the transition season from dry-to-wet the ET regime is most likely water-limited, and the ET anomaly is influenced by the variability of SM, which depends on the phase of
415 the climate driver through precipitation. The SM saturation percentage closely varies with the ITCZ position.

The analysed phenomena have implications for the relationship between SM and heat extremes, gross primary production, irrigation requirements, the carbon and energy cycles and can potentially be used for predicting the response of ecosystems' activity. The chain can be mainly applicable – but not exclusively – to other tropical regions worldwide.

Code availability. We coded scripts in R (<https://www.R-project.org/>) to perform the analysis of the datasets (Duque-Gardeazabal, 2025).
420 They can be consulted at: https://github.com/nduqueg/ET_var_SAme

Data availability. Extended Reconstructed SST version 5 (Huang et al., 2017) is available at: <https://www.ncei.noaa.gov/pub/data/cmb/ersst/v5/netcdf/>. Hadley Center Sea Ice and SST version 4.0.1 (Kennedy et al., 2019) is available at: <https://www.metoffice.gov.uk/hadobs/hadsst4/data/download.html>. Mauna Loa CO2 concentrations are available at <https://gml.noaa.gov/ccgg/trends/data.html>. ECMWF ERA5 reanalysis (Hersbach et al., 2020) and the ERA5-Land reanalysis (Muñoz-Sabater et al., 2021) data are available from Copernicus Climate
425 Data Store web portal <https://cds.climate.copernicus.eu>. MSWEP (Beck et al., 2019) is available at: <http://www.gloh2o.org/mswep/>. ESA CCI SM (Gruber et al., 2019) is available at: <https://catalogue.ceda.ac.uk/uuid/ff890589c21f4033803aa550f52c980c>. GLEAM (Martens et al., 2017) is available at: <https://www.gleam.eu/>. EUMETSAT CLARA-A3 (Karlsson et al., 2023) is available at: https://wui.cmsaf.eu/safira/action/viewProduktDetails?fid=40&eid=22277_22492. HydroSHEDS basins are available at: <https://www.hydrosheds.org/products/hydrobasins> (Lehner and Grill, 2013).

430 *Author contributions.* Conceptualization: N.D-G and S.B.; Data Curation: N.D-G, A.R.F.; Formal Analysis: N.D-G; Funding Acquisition: N.D-G, S.B.; Investigation: N.D-G, A.R.F, S.B.; Methodology: N.D-G, A.R.F., S.B.; Project Administration: N.D-G., S.B.; Resources: S.B.; Software: N.D-G; Supervision: S.B.; Validation: N.D-G, A.R.F., S.B.; Visualisation: N.D-G; Writing - original draft: N.D-G; Writing - review and editing: N.D-G, A.R.F., S.B.

Competing interests. The authors declare that they have no conflict of interest.

435 *Acknowledgements.* We thank the anonymous reviewers and the editor for the constructive comments that helped improve the manuscript. N.D-G. was supported by the Federal Commission for Scholarships for Foreign Students through the Swiss Government Excellence Scholarship (ESKAS No. 2022.0563) for the academic year(s) 2022-2024. A.R.F. was funded by the European Union's Horizon 2020 research and innovation program under the Marie Skłodowska-Curie grant No. 894064 (AQUATIC). S.B. acknowledges funding by the Swiss National Science Foundation (10001375). We are grateful with the institutions that gather and freely disseminate the data used in this research, and to
440 Noemi Imfeld, Sonia Dupuis and Adrian Huerta for recommending datasets or coding functions. N.D-G thanks Helena Gardeazabal, Joaquin Duque and friends for the emotional support throughout this research.

References

- Arias, P. A., Martínez, J. A., and Vieira, S. C.: Moisture sources to the 2010–2012 anomalous wet season in northern South America, *Climate Dynamics*, 45, 2861–2884, <https://doi.org/10.1007/s00382-015-2511-7>, 2015.
- 445 Arias, P. A., Martínez, J. A., Mejía, J. D., Pazos, M. J., Espinoza, J. C., and Wongchuig-Correa, S.: Changes in Normalized Difference Vegetation Index in the Orinoco and Amazon River Basins: Links to Tropical Atlantic Surface Temperatures, *Journal of Climate*, 33, 8537–8559, <https://doi.org/10.1175/JCLI-D-19-0696.1>, 2020.
- Arias, P. A., Garreaud, R., Poveda, G., Espinoza, J. C., Molina-Carpio, J., Masiokas, M., Viale, M., Scaff, L., and van Oevelen, P. J.: Hydroclimate of the Andes Part II: Hydroclimate Variability and Sub-Continental Patterns, *Frontiers in Earth Science*, 8, 1–25, <https://doi.org/10.3389/feart.2020.505467>, 2021.
- 450 Baker, J. C., Garcia-Carreras, L., Gloor, M., Marsham, J. H., Buermann, W., Da Rocha, H. R., Nobre, A. D., De Carioca Araujo, A., and Spracklen, D. V.: Evapotranspiration in the Amazon: Spatial patterns, seasonality, and recent trends in observations, reanalysis, and climate models, *Hydrology and Earth System Sciences*, 25, 2279–2300, <https://doi.org/10.5194/hess-25-2279-2021>, 2021.
- Beck, H. E., Wood, E. F., Pan, M., Fisher, C. K., Miralles, D. G., van Dijk, A. I. J. M., McVicar, T. R., and Adler, R. F.: MSWEP V2 Global 3-Hourly 0.1° Precipitation: Methodology and Quantitative Assessment, *Bulletin of the American Meteorological Society*, 100, 473–500, <https://doi.org/10.1175/BAMS-D-17-0138.1>, 2019.
- 455 Beck, H. E., Pan, M., Miralles, D. G., Reichle, R. H., Dorigo, W. A., Hahn, S., Sheffield, J., Karthikeyan, L., Balsamo, G., Parinussa, R. M., van Dijk, A. I. J. M., Du, J., Kimball, J. S., Vergopolan, N., and Wood, E. F.: Evaluation of 18 satellite- and model-based soil moisture products using in situ measurements from 826 sensors, *Hydrology and Earth System Sciences*, 25, 17–40, <https://doi.org/10.5194/hess-25-17-2021>, 2021.
- 460 Brönnimann, S., Fischer, A. M., Rozanov, E., Poli, P., Compo, G. P., and Sardeshmukh, P. D.: Southward shift of the northern tropical belt from 1945 to 1980, *Nature Geoscience*, 8, 969–974, <https://doi.org/10.1038/ngeo2568>, 2015.
- Cai, W., Wu, L., Lengaigne, M., Li, T., McGregor, S., Kug, J. S., Yu, J. Y., Stuecker, M. F., Santoso, A., Li, X., Ham, Y. G., Chikamoto, Y., Ng, B., McPhaden, M. J., Du, Y., Dommengat, D., Jia, F., Kajtar, J. B., Keenlyside, N., Lin, X., Luo, J. J., Martín-Rey, M., Ruprich-Robert, Y., Wang, G., Xie, S. P., Yang, Y., Kang, S. M., Choi, J. Y., Gan, B., Kim, G. I., Kim, C. E., Kim, S., Kim, J. H., and Chang, P.: Pantropical climate interactions, *Science*, 363, <https://doi.org/10.1126/science.aav4236>, 2019.
- 465 Cai, W., McPhaden, M. J., Grimm, A. M., Rodrigues, R. R., Taschetto, A. S., Garreaud, R. D., Dewitte, B., Poveda, G., Ham, Y. G., Santoso, A., Ng, B., Anderson, W., Wang, G., Geng, T., Jo, H. S., Marengo, J. A., Alves, L. M., Osman, M., Li, S., Wu, L., Karamperidou, C., Takahashi, K., and Vera, C.: Climate impacts of the El Niño–Southern Oscillation on South America, *Nature Reviews Earth and Environment*, 1, 215–231, <https://doi.org/10.1038/s43017-020-0040-3>, 2020.
- 470 Casselman, J. W., Lübbecke, J. F., Bayr, T., Huo, W., Wahl, S., and Domeisen, D. I. V.: The teleconnection of extreme El Niño–Southern Oscillation (ENSO) events to the tropical North Atlantic in coupled climate models, *Weather and Climate Dynamics*, 4, 471–487, <https://doi.org/10.5194/wcd-4-471-2023>, 2023.
- Chang, P., Fang, Y., Saravanan, R., Ji, L., and Seidel, H.: The cause of the fragile relationship between the Pacific El Niño and the Atlantic Niño, *Nature*, 443, 324–328, <https://doi.org/10.1038/nature05053>, 2006.
- 475 Chiang, J. C., Kushnir, Y., and Giannini, A.: Deconstructing Atlantic Intertropical Convergence Zone variability: Influence of the local cross-equatorial sea surface temperature gradient and remote forcing from the Eastern Equatorial Pacific, *Journal of Geophysical Research Atmospheres*, 107, <https://doi.org/10.1029/2000jd000307>, 2002.

- Compo, G. P. and Sardeshmukh, P. D.: Removing ENSO-related variations from the climate record, *Journal of Climate*, 23, 1957–1978, <https://doi.org/10.1175/2009JCLI2735.1>, 2010.
- 480 D’Acunha, B., Dalmagro, H., Zanella de Arruda, P., Biudes, M., Lathuillière, M., Uribe, M., Couto, E., Brando, P., Vourlitis, G., and Johnson, M.: Changes in evapotranspiration, transpiration and evaporation across natural and managed landscapes in the Amazon, Cerrado and Pantanal biomes, *Agricultural and Forest Meteorology*, 346, 109 875, <https://doi.org/10.1016/j.agrformet.2023.109875>, 2024.
- Dominguez, F., Eiras-Barca, J., Yang, Z., Bock, D., Nieto, R., and Gimeno, L.: Amazonian Moisture Recycling Revisited Using WRF With
485 Water Vapor Tracers, *Journal of Geophysical Research: Atmospheres*, 127, <https://doi.org/10.1029/2021JD035259>, 2022.
- Drumond, A., Marengo, J., Ambrizzi, T., Nieto, R., Moreira, L., and Gimeno, L.: The role of the Amazon Basin moisture in the atmospheric branch of the hydrological cycle: A Lagrangian analysis, *Hydrology and Earth System Sciences*, 18, 2577–2598, <https://doi.org/10.5194/hess-18-2577-2014>, 2014.
- Duque-Gardeazabal: An Atlantic influence on evaporation in the Orinoco and Amazon basins - codes,
490 <https://doi.org/10.5281/zenodo.15389246>, 2025.
- Eagleson, P. S.: Ecohydrology: Darwinian expression of vegetation form and function, vol. 53, <https://doi.org/10.1017/CBO9781107415324.004>, 2013.
- ECMWF: IFS Documentation CY48R1 - Part IV: Physical Processes, in: IFS Documentation CY48R1, <https://doi.org/10.21957/02054f0fbf>, 2023.
- 495 Enfield, D. B.: Relationships of inter-American rainfall to tropical Atlantic and Pacific SST variability, *Geophysical Research Letters*, 23, 3305–3308, <https://doi.org/10.1029/96GL03231>, 1996.
- Espinoza, J. C., Ronchail, J., Guyot, J. L., Junquas, C., Vauchel, P., Lavado, W., Drapeau, G., and Pombosa, R.: Climate variability and extreme drought in the upper Solimões River (western Amazon Basin): Understanding the exceptional 2010 drought, *Geophysical Research Letters*, 38, n/a–n/a, <https://doi.org/10.1029/2011GL047862>, 2011.
- 500 Fernandes, K., Giannini, A., Verchot, L., Baethgen, W., and Pinedo-Vasquez, M.: Decadal covariability of Atlantic SSTs and western Amazon dry-season hydroclimate in observations and CMIP5 simulations, *Geophysical Research Letters*, 42, 6793–6801, <https://doi.org/10.1002/2015GL063911>, 2015.
- Friedman, A. R., Hegerl, G. C., Schurer, A. P., Lee, S. Y., Kong, W., Cheng, W., and Chiang, J. C.: Forced and unforced decadal behavior of the interhemispheric SST contrast during the instrumental period (1881–2012): Contextualizing the late 1960s–early 1970s shift, *Journal*
505 *of Climate*, 33, 3487–3509, <https://doi.org/10.1175/JCLI-D-19-0102.1>, 2020.
- García-Serrano, J., Cassou, C., Douville, H., Giannini, A., and Doblas-Reyes, F. J.: Revisiting the ENSO teleconnection to the tropical North Atlantic, *Journal of Climate*, 30, 6945–6957, <https://doi.org/10.1175/JCLI-D-16-0641.1>, 2017.
- Garreaud, R. D., Vuille, M., Compagnucci, R., and Marengo, J.: Present-day South American climate, *Palaeogeography, Palaeoclimatology, Palaeoecology*, 281, 180–195, <https://doi.org/10.1016/j.palaeo.2007.10.032>, 2009.
- 510 Gebrechorkos, S. H., Leyland, J., Dadson, S. J., Cohen, S., Slater, L., Wortmann, M., Ashworth, P. J., Bennett, G. L., Boothroyd, R., Cloke, H., Delorme, P., Griffith, H., Hardy, R., Hawker, L., McLelland, S., Neal, J., Nicholas, A., Tatem, A. J., Vahidi, E., Liu, Y., Sheffield, J., Parsons, D. R., and Darby, S. E.: Global-scale evaluation of precipitation datasets for hydrological modelling, *Hydrology and Earth System Sciences*, 28, 3099–3118, <https://doi.org/10.5194/hess-28-3099-2024>, 2024.
- Grimm, A. M. and Zilli, M. T.: Interannual variability and seasonal evolution of summer monsoon rainfall in South America, *Journal of*
515 *Climate*, 22, 2257–2275, <https://doi.org/10.1175/2008JCLI2345.1>, 2009.

- Gruber, A., Scanlon, T., van der Schalie, R., Wagner, W., and Dorigo, W.: Evolution of the ESA CCI Soil Moisture climate data records and their underlying merging methodology, *Earth System Science Data*, 11, 717–739, <https://doi.org/10.5194/essd-11-717-2019>, 2019.
- Gu, G. and Adler, R. F.: Interannual variability of boreal summer rainfall in the equatorial Atlantic, *International Journal of Climatology*, 29, 175–184, <https://doi.org/10.1002/joc.1724>, 2009.
- 520 Hasler, N. and Avissar, R.: What Controls Evapotranspiration in the Amazon Basin?, *Journal of Hydrometeorology*, 8, 380–395, <https://doi.org/10.1175/JHM587.1>, 2007.
- He, C., Clement, A. C., Kramer, S. M., Cane, M. A., Klavans, J. M., Fenske, T. M., and Murphy, L. N.: Tropical Atlantic multidecadal variability is dominated by external forcing, *Nature*, 622, <https://doi.org/10.1038/s41586-023-06489-4>, 2023.
- Hersbach, H., Bell, B., Berrisford, P., Hirahara, S., Horányi, A., Muñoz-Sabater, J., Nicolas, J., Peubey, C., Radu, R., Schepers, D., Sim-
mons, A., Soci, C., Abdalla, S., Abellan, X., Balsamo, G., Bechtold, P., Biavati, G., Bidlot, J., Bonavita, M., De Chiara, G., Dahlgren,
525 P., Dee, D., Diamantakis, M., Dragani, R., Flemming, J., Forbes, R., Fuentes, M., Geer, A., Haimberger, L., Healy, S., Hogan, R. J.,
Hólm, E., Janisková, M., Keeley, S., Laloyaux, P., Lopez, P., Lupu, C., Radnoti, G., de Rosnay, P., Rozum, I., Vamborg, F., Vil-
laume, S., and Thépaut, J. N.: The ERA5 global reanalysis, *Quarterly Journal of the Royal Meteorological Society*, 146, 1999–2049,
<https://doi.org/10.1002/qj.3803>, 2020.
- 530 Hirschi, M., Mueller, B., Dorigo, W., and Seneviratne, S. I.: Using remotely sensed soil moisture for land-atmosphere cou-
pling diagnostics: The role of surface vs. root-zone soil moisture variability, *Remote Sensing of Environment*, 154, 246–252,
<https://doi.org/10.1016/j.rse.2014.08.030>, 2014.
- Hoyos, I., Cañón-Barriga, J., Arenas-Suárez, T., Dominguez, F., and Rodríguez, B. A.: Variability of regional atmospheric moisture over
Northern South America: patterns and underlying phenomena, *Climate Dynamics*, 52, 893–911, [https://doi.org/10.1007/s00382-018-4172-](https://doi.org/10.1007/s00382-018-4172-9)
535 9, 2019.
- Hua, W., Dai, A., Zhou, L., Qin, M., and Chen, H.: An Externally Forced Decadal Rainfall Seesaw Pattern Over the Sahel and Southeast
Amazon, *Geophysical Research Letters*, 46, 923–932, <https://doi.org/10.1029/2018GL081406>, 2019.
- Huang, B., Thorne, P. W., Banzon, V. F., Boyer, T., Chepurin, G., Lawrimore, J. H., Menne, M. J., Smith, T. M., Vose, R. S., and Zhang,
H. M.: Extended reconstructed Sea surface temperature, Version 5 (ERSSTv5): Upgrades, validations, and intercomparisons, *Journal of*
540 *Climate*, 30, 8179–8205, <https://doi.org/10.1175/JCLI-D-16-0836.1>, 2017.
- Humphrey, V., Berg, A., Ciais, P., Gentile, P., Jung, M., Reichstein, M., Seneviratne, S. I., and Frankenberg, C.: Soil moisture–atmosphere
feedback dominates land carbon uptake variability, *Nature*, 592, 65–69, <https://doi.org/10.1038/s41586-021-03325-5>, 2021.
- IPCC: Climate Change 2021: The Physical Science Basis, Cambridge University Press, Cambridge, United Kingdom,
<https://doi.org/10.1017/9781009157896>, 2021.
- 545 Jarvis, P.: The interpretation of the variations in leaf water potential and stomatal conductance found in canopies in the field, *Philosophical*
Transactions of the Royal Society of London. B, Biological Sciences, 273, 593–610, <https://doi.org/10.1098/rstb.1976.0035>, 1976.
- Jung, M., Koirala, S., Weber, U., Ichii, K., Gans, F., Camps-Valls, G., Papale, D., Schwalm, C., Tramontana, G., and Reichstein, M.: The
FLUXCOM ensemble of global land-atmosphere energy fluxes, *Scientific Data*, 6, 74, <https://doi.org/10.1038/s41597-019-0076-8>, 2019.
- Karlsson, K.-G., Riihelä, A., Trentmann, J., Stengel, M., Solodovnik, I., Meirink, J. F., Devasthale, A., Jääskeläinen, E., Kallio-Myers,
550 V., Eliasson, S., Benas, N., Johansson, E., Stein, D., Finkensieper, S., Håkansson, N., Akkermans, T., Clerbaux, N., Selbach, N.,
Marc, S., and Hollmann, R.: CLARA-A3: CM SAF cLoud, Albedo and surface RAdiation dataset from AVHRR data - Edition 3,
https://doi.org/10.5676/EUM_SAF_CM/CLARA_AVHRR/V003, 2023.

- Kaune, A., Werner, M., López López, P., Rodríguez, E., Karimi, P., and De Fraiture, C.: Can global precipitation datasets benefit the estimation of the area to be cropped in irrigated agriculture?, *Hydrology and Earth System Sciences*, 23, 2351–2368, <https://doi.org/10.5194/hess-23-2351-2019>, 2019.
- Kennedy, J. J., Rayner, N. A., Atkinson, C. P., and Killick, R. E.: An Ensemble Data Set of Sea Surface Temperature Change From 1850: The Met Office Hadley Centre HadSST.4.0.0.0 Data Set, *Journal of Geophysical Research: Atmospheres*, 124, 7719–7763, <https://doi.org/10.1029/2018JD029867>, 2019.
- Le, T. and Bae, D.-H.: Response of global evaporation to major climate modes in historical and future Coupled Model Intercomparison Project Phase 5 simulations, *Hydrology and Earth System Sciences*, 24, 1131–1143, <https://doi.org/10.5194/hess-24-1131-2020>, 2020.
- Lehner, B. and Grill, G.: Global river hydrography and network routing: baseline data and new approaches to study the world’s large river systems, *Hydrological Processes*, 27, 2171–2186, <https://doi.org/10.1002/hyp.9740>, 2013.
- Lian, X., Morfopoulos, C., and Gentine, P.: Water deficit and storm disturbances co-regulate Amazon rainforest seasonality, *Science Advances*, 10, <https://doi.org/10.1126/sciadv.adk5861>, 2024.
- Lopes, A. V., Chiang, J. C. H., Thompson, S. A., and Dracup, J. A.: Trend and uncertainty in spatial-temporal patterns of hydrological droughts in the Amazon basin, *Geophysical Research Letters*, 43, 3307–3316, <https://doi.org/10.1002/2016GL067738>, 2016.
- Lübbecke, J. F. and McPhaden, M. J.: On the Inconsistent Relationship between Pacific and Atlantic Niños, *Journal of Climate*, 25, 4294–4303, <https://doi.org/10.1175/JCLI-D-11-00553.1>, 2012.
- Lübbecke, J. F., Rodríguez-Fonseca, B., Richter, I., Martín-Rey, M., Losada, T., Polo, I., and Keenlyside, N. S.: Equatorial Atlantic variability—Modes, mechanisms, and global teleconnections, *Wiley Interdisciplinary Reviews: Climate Change*, 9, 1–18, <https://doi.org/10.1002/wcc.527>, 2018.
- Makarieva, A. M., Nefiodov, A. V., Nobre, A. D., Baudena, M., Bardi, U., Sheil, D., Saleska, S. R., Molina, R. D., and Rammig, A.: The role of ecosystem transpiration in creating alternate moisture regimes by influencing atmospheric moisture convergence, *Global Change Biology*, 29, 2536–2556, <https://doi.org/10.1111/gcb.16644>, 2023.
- Marengo, J. A. and Espinoza, J. C.: Extreme seasonal droughts and floods in Amazonia: Causes, trends and impacts, *International Journal of Climatology*, 36, 1033–1050, <https://doi.org/10.1002/joc.4420>, 2016.
- Mariotti, A., Ruti, P. M., and Rixen, M.: Progress in subseasonal to seasonal prediction through a joint weather and climate community effort, *npj Climate and Atmospheric Science*, 1, 2–5, <https://doi.org/10.1038/s41612-018-0014-z>, 2018.
- Martens, B., Miralles, D. G., Lievens, H., Van Der Schalie, R., De Jeu, R. A., Fernández-Prieto, D., Beck, H. E., Dorigo, W. A., and Verhoest, N. E.: GLEAM v3: Satellite-based land evaporation and root-zone soil moisture, *Geoscientific Model Development*, 10, 1903–1925, <https://doi.org/10.5194/gmd-10-1903-2017>, 2017.
- Martens, B., Waegeman, W., Dorigo, W. A., Verhoest, N. E. C., and Miralles, D. G.: Terrestrial evaporation response to modes of climate variability, *npj Climate and Atmospheric Science*, 1, 43, <https://doi.org/10.1038/s41612-018-0053-5>, 2018.
- Martín-Rey, M., Rodríguez-Fonseca, B., Polo, I., and Kucharski, F.: On the Atlantic–Pacific Niños connection: a multidecadal modulated mode, *Climate Dynamics*, 43, 3163–3178, <https://doi.org/10.1007/s00382-014-2305-3>, 2014.
- Merz, B., Blöschl, G., Vorogushyn, S., Dottori, F., Aerts, J. C., Bates, P., Bertola, M., Kemter, M., Kreibich, H., Lall, U., and Macdonald, E.: Causes, impacts and patterns of disastrous river floods, *Nature Reviews Earth and Environment*, 2, 592–609, <https://doi.org/10.1038/s43017-021-00195-3>, 2021.

Miralles, D. G., Van Den Berg, M. J., Gash, J. H., Parinussa, R. M., De Jeu, R. A., Beck, H. E., Holmes, T. R., Jiménez, C., Verhoest, N. E.,
590 Dorigo, W. A., Teuling, A. J., and Johannes Dolman, A.: El Niño-La Niña cycle and recent trends in continental evaporation, *Nature Climate Change*, 4, 122–126, <https://doi.org/10.1038/nclimate2068>, 2014.

Mishra, A. K. and Singh, V. P.: A review of drought concepts, *Journal of Hydrology*, 391, 202–216, <https://doi.org/10.1016/j.jhydrol.2010.07.012>, 2010.

Moura, M. M., dos Santos, A. R., Pezzopane, J. E. M., Alexandre, R. S., da Silva, S. F., Pimentel, S. M., de Andrade, M. S. S., Silva,
595 F. G. R., Branco, E. R. F., Moreira, T. R., da Silva, R. G., and de Carvalho, J. R.: Relation of El Niño and La Niña phenomena to precipitation, evapotranspiration and temperature in the Amazon basin, *Science of the Total Environment*, 651, 1639–1651, <https://doi.org/10.1016/j.scitotenv.2018.09.242>, 2019.

Münnich, M. and Neelin, J. D.: Seasonal influence of ENSO on the Atlantic ITCZ and equatorial South America, *Geophysical Research Letters*, 32, <https://doi.org/10.1029/2005GL023900>, 2005.

600 Muñoz-Sabater, J., Dutra, E., Agustí-Panareda, A., Albergel, C., Arduini, G., Balsamo, G., Boussetta, S., Choulga, M., Harrigan, S., Hersbach, H., Martens, B., Miralles, D. G., Piles, M., Rodríguez-Fernández, N. J., Zsoter, E., Buontempo, C., and Thépaut, J. N.: ERA5-Land: A state-of-the-art global reanalysis dataset for land applications, *Earth System Science Data*, 13, 4349–4383, <https://doi.org/10.5194/essd-13-4349-2021>, 2021.

Nemani, R. R., Keeling, C. D., Hashimoto, H., Jolly, W. M., Piper, S. C., Tucker, C. J., Myneni, R. B., and Running,
605 S. W.: Climate-Driven Increases in Global Terrestrial Net Primary Production from 1982 to 1999, *Science*, 300, 1560–1563, <https://doi.org/10.1126/science.1082750>, 2003.

O'Connor, J., Santos, M. J., Rebel, K. T., and Dekker, S. C.: The influence of water table depth on evapotranspiration in the Amazon arc of deforestation, *Hydrology and Earth System Sciences*, 23, 3917–3931, <https://doi.org/10.5194/hess-23-3917-2019>, 2019.

Olmo, M. E., Espinoza, J. C., Bettolli, M. L., Sierra, J. P., Junquas, C., Arias, P. A., Moron, V., and Balmaceda-Huarte, R.: Circulation
610 Patterns and Associated Rainfall Over South Tropical South America: GCMs Evaluation During the Dry-To-Wet Transition Season, *Journal of Geophysical Research: Atmospheres*, 127, <https://doi.org/10.1029/2022JD036468>, 2022.

Pabón, J. and Dorado, J.: INTRASEASONAL VARIABILITY OF RAINFALL OVER NORTHERN SOUTH AMERICA AND CARIBBEAN REGION, *Earth Sciences Research Journal*, 12, 194–212, 2008.

Paccini, L., Hohenegger, C., and Stevens, B.: Explicit versus Parameterized Convection in Response to the Atlantic Meridional Mode, *Journal*
615 *of Climate*, 34, 3343–3354, <https://doi.org/10.1175/JCLI-D-20-0224.1>, 2021.

Poveda, G., Jaramillo, A., Gil, M. M., Quiceno, N., and Mantilla, R. I.: Seasonally in ENSO-related precipitation, river discharges, soil moisture, and vegetation index in Colombia, *Water Resources Research*, 37, 2169–2178, <https://doi.org/10.1029/2000WR900395>, 2001.

Poveda, G., Waylen, P. R., and Pulwarty, R. S.: Annual and inter-annual variability of the present climate in northern South America and southern Mesoamerica, *Palaeogeography, Palaeoclimatology, Palaeoecology*, 234, 3–27, <https://doi.org/10.1016/j.palaeo.2005.10.031>,
620 2006.

Roberts, J. M., Gash, J. H. C., Tani, M., and Bruijnzeel, L. A.: Controls on evaporation in lowland tropical rainforest, in: *Forests, Water and People in the Humid Tropics*, pp. 287–313, Cambridge University Press, <https://doi.org/10.1017/CBO9780511535666.019>, 2005.

Rodrigues, R. R. and McPhaden, M. J.: Why did the 2011–2012 La Niña cause a severe drought in the Brazilian Northeast?, *Geophysical Research Letters*, 41, 1012–1018, <https://doi.org/10.1002/2013GL058703>, 2014.

- 625 Ronchail, J., Cochonneau, G., Molinier, M., Guyot, J. L., De Miranda Chaves, A. G., Guimarães, V., and De Oliveira, E.: Interannual rainfall variability in the Amazon basin and sea-surface temperatures in the equatorial Pacific and the tropical Atlantic Oceans, *International Journal of Climatology*, 22, 1663–1686, <https://doi.org/10.1002/joc.815>, 2002.
- Ruiz-Barradas, A., Carton, J. A., and Nigam, S.: Structure of Interannual-to-Decadal climate variability in the tropical Atlantic sector, *Journal of Climate*, 13, 3285–3297, [https://doi.org/10.1175/1520-0442\(2000\)013<3285:SOITDC>2.0.CO;2](https://doi.org/10.1175/1520-0442(2000)013<3285:SOITDC>2.0.CO;2), 2000.
- 630 Ruiz-Vásquez, M., Arias, P. A., and Martínez, J. A.: Enso influence on water vapor transport and thermodynamics over Northwestern South America, *Theoretical and Applied Climatology*, 155, 3771–3789, <https://doi.org/10.1007/s00704-024-04848-3>, 2024.
- Seneviratne, S. I., Corti, T., Davin, E. L., Hirschi, M., Jaeger, E. B., Lehner, I., Orlowsky, B., and Teuling, A. J.: Investigating soil moisture-climate interactions in a changing climate: A review, *Earth-Science Reviews*, 99, 125–161, <https://doi.org/10.1016/j.earscirev.2010.02.004>, 2010.
- 635 Staal, A., Tuinenburg, O. A., Bosmans, J. H. C., Holmgren, M., van Nes, E. H., Scheffer, M., Zemp, D. C., and Dekker, S. C.: Forest-rainfall cascades buffer against drought across the Amazon, *Nature Climate Change*, 8, 539–543, <https://doi.org/10.1038/s41558-018-0177-y>, 2018.
- Thoning, K. W., Tans, P. P., and Komhyr, W. D.: Atmospheric carbon dioxide at Mauna Loa Observatory: 2. Analysis of the NOAA GMCC data, 1974–1985, *Journal of Geophysical Research: Atmospheres*, 94, 8549–8565, <https://doi.org/10.1029/JD094iD06p08549>, 1989.
- 640 Torralba, V., Rodríguez-Fonseca, B., Mohino, E., and Losada, T.: The non-stationary influence of the Atlantic and Pacific niños on north Eastern South American rainfall, *Frontiers in Earth Science*, 3, 1–10, <https://doi.org/10.3389/feart.2015.00055>, 2015.
- Towner, J., Ficchi, A., Cloke, H. L., Bazo, J., Coughlan de Perez, E., and Stephens, E. M.: Influence of ENSO and tropical Atlantic climate variability on flood characteristics in the Amazon basin, *Hydrology and Earth System Sciences*, 25, 3875–3895, <https://doi.org/10.5194/hess-25-3875-2021>, 2021.
- 645 Ummenhofer, C. C. and Meehl, G. A.: Extreme weather and climate events with ecological relevance: a review, *Philosophical Transactions of the Royal Society B: Biological Sciences*, 372, 20160 135, <https://doi.org/10.1098/rstb.2016.0135>, 2017.
- Valencia, S., Marín, D. E., Gómez, D., Hoyos, N., Salazar, J. F., and Villegas, J. C.: Spatio-temporal assessment of Gridded precipitation products across topographic and climatic gradients in Colombia, *Atmospheric Research*, 285, 106 643, <https://doi.org/10.1016/j.atmosres.2023.106643>, 2023.
- 650 Vallès-Casanova, I., Lee, S., Foltz, G. R., and Pelegrí, J. L.: On the Spatiotemporal Diversity of Atlantic Niño and Associated Rainfall Variability Over West Africa and South America, *Geophysical Research Letters*, 47, 1–10, <https://doi.org/10.1029/2020GL087108>, 2020.
- van der Ent, R. J. and Savenije, H. H. G.: Length and time scales of atmospheric moisture recycling, *Atmospheric Chemistry and Physics*, 11, 1853–1863, <https://doi.org/10.5194/acp-11-1853-2011>, 2011.
- Wang, K. and Dickinson, R. E.: A review of global terrestrial evapotranspiration: Observation, modeling, climatology, and climatic variability, *Reviews of Geophysics*, 50, 1–54, <https://doi.org/10.1029/2011RG000373>, 2012.
- 655 Wang-Erlandsson, L., Fetzer, I., Keys, P. W., van der Ent, R. J., Savenije, H. H. G., and Gordon, L. J.: Remote land use impacts on river flows through atmospheric teleconnections, *Hydrology and Earth System Sciences*, 22, 4311–4328, <https://doi.org/10.5194/hess-22-4311-2018>, 2018.
- Williams, I. N. and Patricola, C. M.: Diversity of ENSO Events Unified by Convective Threshold Sea Surface Temperature: A Nonlinear ENSO Index, *Geophysical Research Letters*, 45, 9236–9244, <https://doi.org/10.1029/2018GL079203>, 2018.
- 660

- Xie, Z., Yao, Y., Tang, Q., Liu, M., Fisher, J. B., Chen, J., Zhang, X., Jia, K., Li, Y., Shang, K., Jiang, B., Yang, J., Yu, R., Zhang, X., Guo, X., Liu, L., Ning, J., Fan, J., and Zhang, L.: Evaluation of seven satellite-based and two reanalysis global terrestrial evapotranspiration products, *Journal of Hydrology*, 630, 130 649, <https://doi.org/10.1016/j.jhydrol.2024.130649>, 2024.
- Yoon, J. H. and Zeng, N.: An Atlantic influence on Amazon rainfall, *Climate Dynamics*, 34, 249–264, <https://doi.org/10.1007/s00382-009-0551-6>, 2010.
- Zanin, P. R., Pareja-Quispe, D., and Espinoza, J.-c.: Evapotranspiration in the Amazon Basin: Couplings, hydrological memory and water feedback, *Agricultural and Forest Meteorology*, 352, 110 040, <https://doi.org/10.1016/j.agrformet.2024.110040>, 2024.
- Zemp, D. C., Schleussner, C.-F., Barbosa, H. M. J., van der Ent, R. J., Donges, J. F., Heinke, J., Sampaio, G., and Rammig, A.: On the importance of cascading moisture recycling in South America, *Atmospheric Chemistry and Physics*, 14, 13 337–13 359, <https://doi.org/10.5194/acp-14-13337-2014>, 2014.
- Zhang, Y., Peña-Arancibia, J. L., McVicar, T. R., Chiew, F. H., Vaze, J., Liu, C., Lu, X., Zheng, H., Wang, Y., Liu, Y. Y., Miralles, D. G., and Pan, M.: Multi-decadal trends in global terrestrial evapotranspiration and its components, *Scientific Reports*, 6, 1–12, <https://doi.org/10.1038/srep19124>, 2016.
- Zhao, M. and Running, S. W.: Drought-Induced Reduction in Global Terrestrial Net Primary Production from 2000 Through 2009, *Science*, 329, 940–943, <https://doi.org/10.1126/science.1192666>, 2010.